

Electromagnetic calorimetry with lead fluoride crystals

R.D. Appuhn^{a,1}, F. Brasse^b, T. Deckers^a, H. Kolanoski^a, V. Korbel^b, A. Lindner^{a,*}, K. Meier^{b,2},
S. Spielmann^a, S. Valkar^c, A. Walther^a, D. Wegener^a

^a *Institut für Physik, Universität, Dortmund, Germany*

^b *DESY, Hamburg, Germany*

^c *Nuclear Center, Charles University, Praha, Czech Republic*

Received 3 June 1994

The properties of four PbF₂ crystals of size 21 × 21 × 175 mm³ were studied with electron and pion beams in the energy range from 1 to 6 GeV. An energy resolution for electrons of 6.3%/√*E*/GeV was achieved with a 2 × 2 matrix of four PbF₂ crystals, which corresponds to 5.6%/√*E*/GeV when corrected for lateral leakage by Monte Carlo simulations. The deviation from linearity was smaller than 0.5%. The time resolution was found to be better than 0.6 ns. We studied also optical properties, radiation hardness, position resolution and spatial homogeneity. An efficient separation of electromagnetic and hadronic showers was achieved.

1. Introduction

The H1 collaboration intends to upgrade the H1 detector at HERA with a new backward calorimeter to measure energy and impact point of scattered electrons with high precision down to small angles with respect to the beam-line. Since hadrons are the most frequent particles produced in e⁻p scattering at low *Q*² and in photoproduction events a good separation capability between electromagnetic and hadronic showers is required. Hence a very compact calorimeter is needed to minimize the overlap of energy depositions. Excellent time resolution is necessary to suppress proton beam induced background entering the back of the calorimeter. One option was to build the calorimeter out of lead fluoride (PbF₂) crystals and therefore we studied the performance of this material for calorimetry.

PbF₂ crystals have been investigated previously for their use in calorimetry [1–4]. We used PbF₂ in its cubic lattice form as a Cherenkov radiator. It has a very high density (7.77 g/cm³), a short radiation length (9.3 mm) and a small Moliere radius (22 mm). The light output was found to be sufficient to allow a good electromagnetic energy resolution. PbF₂ shows a rather good radiation hardness. Moreover radiation damage can be cured by optical bleaching. Because of the relative cheap raw material lead fluoride crystals are expected to be produced in large quantities at modest costs compared to other crystals.

2. The experimental setup

We performed measurements with four crystals of size 21 × 21 × 175 mm³, which were produced by Optovac, Inc. at Brookfield, MA, USA within a larger sample. The crystal length corresponds to more than 18 radiation lengths. The optical properties of the crystals were measured at the universities of Prague and Dortmund. The response of single crystals as well as that of a 2 × 2 matrix to an e⁻ beam with energies between 1 and 6 GeV was tested at a DESY testbeam in Hamburg. The trigger was defined by a coincidence of two scintillation counters and a veto counter with a 2.5 mm diameter hole in front of the calorimeter. During parts of the data taking a drift chamber was also available, which allowed to reconstruct the impact point on the crystal surface with a precision of 0.5 mm. In this case a veto counter with an 8 mm diameter hole was used. Each crystal was coupled to a fine mesh photomultiplier tube (Hamamatsu R4722) with an UV-glass window and a bialkali photocathode which covered approximately 45% of the crystal surface. We used these tubes because they are able to work in the 1.2 T magnetic field of the H1 detector, and will be used in the upgraded H1 backward calorimeter. Properties of these photomultipliers in high magnetic fields were measured in parallel to the crystal tests [5]. Crystals and phototubes were placed in a light tight box with an entrance window for the beam covered by black tape. The photomultipliers were read out simultaneously by ADCs (10 bit) and TDCs (9 bit) of conventional CAMAC electronics. The width of the pedestal ADC distributions corresponded to a noise term between 10 and 20 MeV.

In addition the 2 × 2 crystal matrix was exposed to

* Corresponding author.

¹ Now at DESY, Hamburg, Germany.

² Now at Institut für-Hochenergiephysik, Universität Heidelberg, Germany.

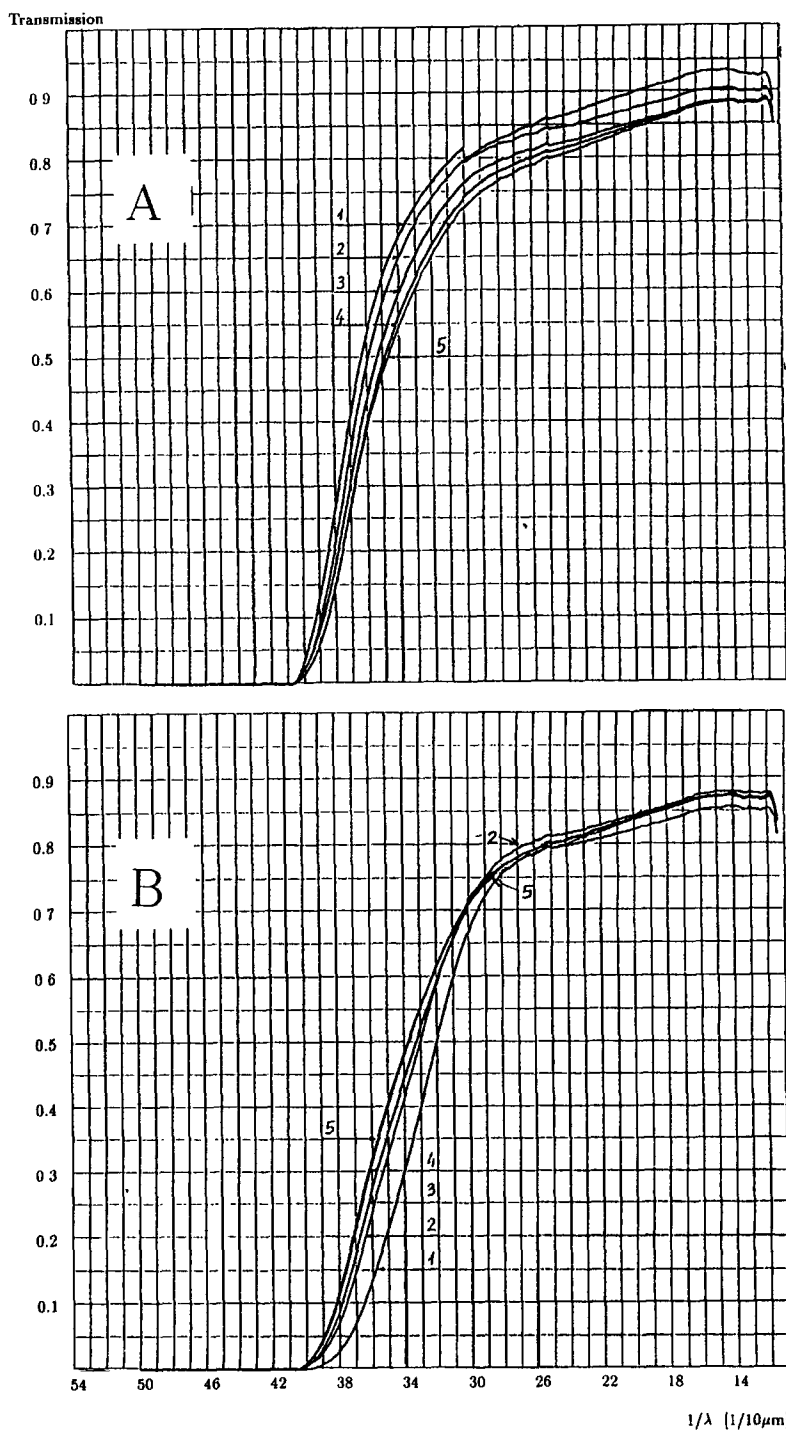


Fig. 1. The transmission as a function of wavelength for light passing the crystal transverse (21 mm) at different positions along the crystal axis: The curves (1) to (5) were recorded at distances of 1 to 5 cm away from the end of the crystal, where the growing process started (A) and where it finished (B). No corrections for reflections at the crystal surfaces were made.

positron and hadron beams (1 to 6 GeV) with a rectangular $10 \times 10 \text{ mm}^2$ beamspot at a PS test beam at CERN. Here we used conventional Phillips XP 2802 and XP 2812 phototubes, as the Hamamatsu tubes were not available at this time.

3. Properties of the crystals

PbF_2 crystals have a compression strength of at least 0.2 tons/cm^2 [2] which allows the stacking of a calorimeter wall without internal support. We measured a Knoop hardness [6] of 27 ± 2 similar to plastic scintillator. The crystals could be easily polished, but care has to be taken to avoid cracking due to internal stresses originating from the thermal growing procedure.

To determine the homogeneity of the four PbF_2 crystals we measured their optical properties as well as the light yield and energy resolution for electromagnetic showers.

3.1. Optical transmission

The transmission of the four PbF_2 crystals as a function of the wavelength was measured transverse to the longitudinal crystal axis. Results for one crystal are shown in Fig. 1. Note that no corrections for reflections at the crystals entrance and exit surfaces have been applied so that direct comparisons with other published results [2,3] can be made. From reflections alone the transmitted light at wavelengths around 400 nm is reduced to an intensity of $\approx 84\%$ of the incident light. All crystals show a decrease of the transmission when the light passes through parts of the crystal grown late in the production process. This effect is rather strong for light with wavelength below 350 nm. For visible light all crystals appear very clear. However they show some scatter centers (presumably lead) near the end, where the growing finished. In one crystal these centers extend over the last third of the crystal. Hence transparency measurements will be important quality tests for a calorimeter.

3.2. Refractive indexes

Table 1 shows refractive indexes for one PbF_2 crystal measured at different wavelengths and two different temperatures. Our results for PbF_2 are in good agreement to the data published in Ref. [2]. The variations of the refractive index with temperature are found to be small and will not affect the performance of lead fluoride in calorimetry. We added measurements of two optical greases used in our tests.

3.3. Radiation damage

A 4.2 mm long PbF_2 crystal piece was irradiated by photons from a ^{60}Co source with a dose of 1.3 Mrad at the

Table 1

Refractive indexes for a PbF_2 crystal and two optical coupling compounds (Dow corning 20-057 and Rhodosil from Rhone Poulence at 25°C)

| λ [nm] | PbF_2 | | Coupl. comp. | |
|----------------|----------------|-------|--------------|----------|
| | 20°C | 80°C | Dow | Rhodosil |
| 400 | 1.815 | 1.812 | 1.444 | 1.414 |
| 450 | 1.801 | 1.798 | 1.439 | 1.414 |
| 500 | 1.786 | 1.783 | 1.433 | 1.407 |
| 550 | 1.773 | 1.770 | 1.429 | – |
| 600 | 1.766 | 1.763 | 1.427 | 1.406 |
| 650 | 1.759 | 1.756 | 1.424 | – |

Nuclear Center in Prague. The transmissions before and after irradiation are shown in Fig. 2. A drastic decrease at short wavelengths is visible, but the radiation damage was cured by exposing the crystal to daylight. Only at very short wavelengths below 280 nm some residual damage persists. After 40 days in the daylight the transmission was even better than measured for the unirradiated crystal at wavelengths above 320 nm. A similar result was noticed already in Ref. [2], where an improvement of the transmission of non-irradiated PbF_2 crystals after exposure to UV light was observed. UV light can possibly heal structure defects from the crystal growing process.

3.4. Light yield and electromagnetic resolution

The number of photoelectrons produced by an electromagnetic shower was estimated with the help of a LED reference source. With the multiplication factor δ for each photomultiplier dynode (calculated from the gain and the number of dynodes) the mean number of photoelectrons N_e is related to the mean amplitude A and the standard deviation σ of the LED signal measured with the photomultiplier by $\sigma/A = \sqrt{\delta/(\delta-1)} / \sqrt{N_e}$ [5]. Comparing

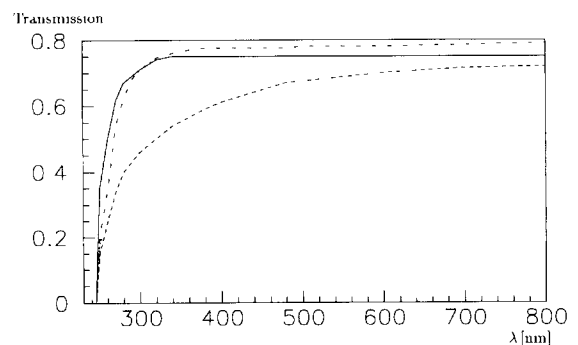


Fig. 2. The transmission of a 4.2 mm thick PbF_2 crystal before (line) and after 1.3 Mrad γ -irradiation from a ^{60}Co source (dashed). The dotted and dashed-dotted curves show the transmission after 3 and 40 days in (winter) daylight, respectively. No corrections for reflections at the crystal surfaces were applied.

Table 2

The relative light yield and energy resolution for the four crystals measured with a 3 GeV electron beam. The resolutions were not corrected for leakage fluctuation

| Crystal | Rel. light yield | Resolution |
|---------|------------------|-------------------|
| No. 1 | 1 | $(5.7 \pm 0.1)\%$ |
| No. 2 | 1.06 ± 0.03 | $(5.6 \pm 0.2)\%$ |
| No. 3 | 1.15 ± 0.03 | $(4.9 \pm 0.2)\%$ |
| No. 4 | 1.00 ± 0.03 | $(5.6 \pm 0.1)\%$ |

the LED signal with the response from an electron beam we found $(1.6 \pm 0.3) \times 10^3$ photoelectrons per GeV, if the Hamamatsu phototubes mentioned above were coupled with optical grease to the crystals. This result is corrected for lateral leakage of the electromagnetic shower (see Section 5.1). No difference between the two optical greases used in our tests was observed.

To compare light yield and energy resolution of the four crystals the same photomultiplier was attached with optical grease to each crystal at the side where the growing process started. The signals from an e^- beam hitting the center of the front face of the crystals were measured and compared. Table 2 shows the results for the relative light yield normalized to the first crystal, and the energy resolution for 3 GeV electrons. Both the mean value and the width of the signals were determined by fitting to the measured ADC spectra a Gaussian with an exponential tail on the left side to account for interaction of electrons before their impact on the PbF_2 . Two examples are given in Fig. 3. Within the experimental uncertainties (mainly due to gain variations of the photomultiplier) all crystals but one show the same light yield and a relative resolution around 5.6% at 3 GeV. Although crystal No. 3 exhibits many scattering centers its transparency to UV light is superior to the other crystals in the test. Consequently it produces 15% more light and achieves a resolution of

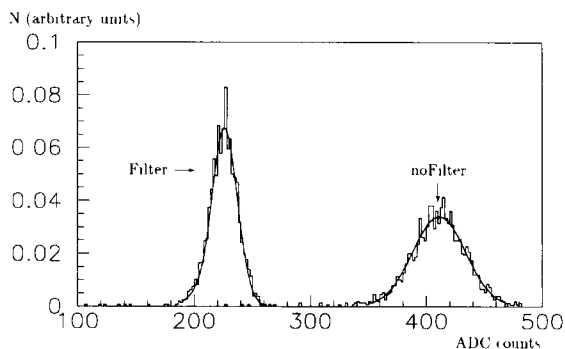


Fig. 3. The measured pedestal subtracted ADC spectra for 3 GeV electrons in one PbF_2 crystal without and with a filter, which transmits light with wavelengths above 375 nm. Both distributions are normalized to the same area. Fits are shown by smooth lines.

Table 3

The light output and resolution (not corrected for leakage fluctuation) for PbF_2 crystals exposed to 3 GeV electrons. The photomultiplier was attached to the opposite end compared to Table 2. The light output is related to the numbers in Table 2

| Crystal | Rel. light yield | Resolution |
|---------|------------------|-------------------|
| No. 1 | 0.90 ± 0.02 | $(4.9 \pm 0.1)\%$ |
| No. 3 | 0.84 ± 0.02 | $(4.7 \pm 0.2)\%$ |
| No. 4 | 0.86 ± 0.02 | $(5.1 \pm 0.1)\%$ |

4.9%. These comparisons indicate that production of many crystals seems possible without too large variations.

Attaching the photomultiplier to the opposite bad transmission end of the crystals resulted in a decrease of the light yield but the resolution improved slightly (Table 3). Due to the limited beam time available we had to skip a measurement of crystal No. 2. The observed behavior may be understood from the optical measurements. When the crystal side with bad transmission is attached to the photomultiplier (Table 3) the light is attenuated independent of spatial shower fluctuations, because only a very small fraction of the electromagnetic shower develops in the last part of the crystal. In the other orientation (Table 2) the shower develops in the part with bad transmission so that the light damping depends on the individual spatial development of the electromagnetic shower. In this case the mean light yield is higher, but additional fluctuations deteriorate the energy resolution.

3.5. Time resolution

A discriminator with a threshold of 30 mV was used to measure the spread of the arrival time of signals from 3 GeV electrons with a typical pulse height of 400 mV and a signal rise time (10% to 90%) of less than 5 ns. A small pulse height correction was applied. Because the time spread of the trigger scintillator was not known our measurement $\sigma(\text{rms}) = 0.6$ ns is only an upper limit for the time resolution of a PbF_2 calorimeter.

4. Optimization of PbF_2 crystals for calorimetry

We studied different crystal wrappings and optical couplings to the photomultiplier to optimize the PbF_2 crystals for energy measurements.

4.1. Wrapping the crystals

The light outputs for different wrap materials are compared in Table 4 normalizing to the result for a wrap with aluminized mylar foil with both crystal ends open. In all measurements the same crystal and the same photomultiplier coupled with optical grease were exposed to 3 GeV

Table 4

The relative light output for a PbF_2 crystal with different wrappings

| Wrap material | Rel. light yield |
|----------------------------|------------------|
| Al. Mylar foil (4 sides) | 1 |
| Al. Mylar foil (5 sides) | 1.05 ± 0.03 |
| White paper (4 sides) | 0.92 ± 0.03 |
| Teflon tape (4 sides) | 0.99 ± 0.03 |
| TiO painted foil (4 sides) | 0.94 ± 0.03 |

electrons. The change due to different wraps is not as strong as for scintillating crystals [7], because the Cherenkov light is emitted mainly in forward direction with respect to the beam axis.

In addition the influence of surface treatments were studied. After aluminizing the four long sides of a crystal the light output decreased to 8% relative to a polished surface, because the light in the crystal was no longer transported by total internal reflection. A roughed uncoated surface reduced the light to 34%.

4.2. Optical coupling

The coupling of a photomultiplier to a crystal by a defined air gap is most stable in time and therefore the most attractive solution for a large detector. We compared the light yield for a coupling via a thin air gap (realized by a $60 \mu\text{m}$ thick distance ring) between PbF_2 crystal and photomultiplier to a coupling with optical grease. The ratio of the mean ADC values for both configurations is found to be $\text{Mean}(\text{air})/\text{Mean}(\text{grease}) = 0.30 \pm 0.01$.

The light yield with an air gap can be increased by roughen the crystal end facing the photomultiplier. This was simulated by attaching a 3 mm thick PbF_2 plate with optical grease to the crystal, where the end facing the photomultiplier was roughed. With an air gap between phototube and roughed plate we obtained $\text{Mean}(\text{air,rough})/\text{Mean}(\text{grease}) = 0.43 \pm 0.01$, which is 40% higher than observed with an air gap and polished end face.

To reduce the influence of radiation damage and spatial variations of the transmission in the crystal on energy measurements we suppressed UV light of the Cherenkov spectrum, as both effects are most pronounced at wavelengths below 400 nm. 3 GeV electrons were measured with one crystal (without radiation damage), where a filter (Schott GG375) was placed between crystal and phototube attached to the end with good transmission. Filter and phototube were both coupled with optical grease. Only light with wavelengths above 375 nm could pass the filter. Although the filter reduced the light yield to $(55 \pm 2)\%$ the resolution improved by $(10 \pm 5)\%$ relative to measurements without filter (see Fig. 3).

5. Measurements with a 2×2 PbF_2 matrix

Four PbF_2 crystals were wrapped in aluminized mylar foil, arranged in a 2×2 matrix and coupled with optical grease to the Hamamatsu photomultipliers for measurements at the DESY testbeam. The CERN data were recorded with wraps of white paper and air gaps between the crystals and the Phillips photomultipliers. The signals of the four phototubes were calibrated relative to each other using the electron beams.

5.1. Linearity and energy resolution

The impact point of the beam was placed on the center of one crystal. For this measurement the whole matrix was tilted by 5° both horizontally and vertically with respect to the beam axis such that the shower is better contained in the PbF_2 calorimeter. Fig. 4 shows the sum of the four photomultiplier signals for e^- energies of 2, 4 and 6 GeV as examples. We fitted the same modified Gaussian as described in Section 3.4. Mean values and widths of the Gaussian were used in the following comparisons.

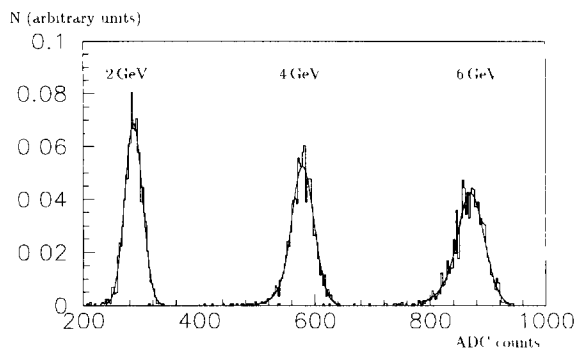


Fig. 4. The sum of the signals of the four crystals for electrons of 2, 4 and 6 GeV hitting the center area of one of the PbF_2 crystals. All distributions are normalized to the same area. Fits are shown by smooth lines.

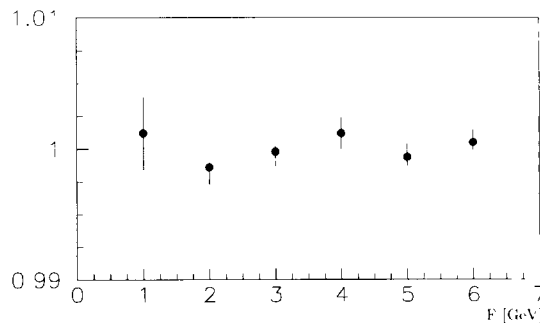


Fig. 5. The deviation from linearity for electron energies measured in the PbF_2 matrix.

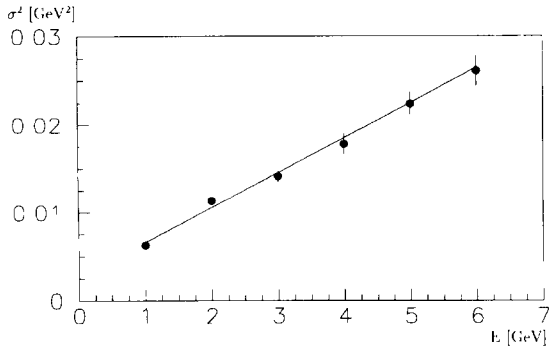


Fig. 6. The resolution squared for different electron energies and a straight-line fit to the data.

The deviation from linearity is shown in Fig. 5, where the residuals are shown as a function of the beam energy. The deviation is smaller than 0.5% in the energy range from 1 to 6 GeV. The square of the measured energy resolution is plotted in Fig. 6 as a function of the electron energy. The distribution can be fitted by a straight line ($\sigma^2 = a^2 + b^2 E$). We obtained a noise-like term $a = (51 \pm 5)$ MeV, which is consistent with the expectation from the momentum spread of the DESY testbeam and the fluctuations of the ADC pedestals. The Poisson term was found to be $b = (6.31 \pm 0.16)\% \text{ GeV}^{1/2}$.

The energy resolution is deteriorated by fluctuations of the deposited energy, as our matrix with a lateral size of $42 \times 42 \text{ mm}^2$ does not contain the full electromagnetic shower. Simulations with EGS show that for the impact point and beam spot size used 86% of the energy is deposited in the PbF_2 matrix with corresponding fluctuations of $\sigma_{\text{leak}} = (3.0 \pm 0.2)\% \text{ GeV}^{1/2}$, where the error is due to systematic uncertainties. The longitudinal leakage of our 18 radiation lengths long calorimeter is much smaller than the lateral leakage at low test beam energies and will be neglected in the following discussion. For measurements of 30 GeV electrons, however, crystals at least 25 radiation lengths long should be used to limit fluctuations from longitudinal leakage to less than 0.5% $\text{GeV}^{1/2}$.

Subtracting the lateral leakage fluctuations quadratically from our measurements we obtain the electromagnetic energy resolution

$$\frac{\sigma}{E} = \frac{(5.6 \pm 0.2)\%}{\sqrt{E/\text{GeV}}}.$$

Our result is in good agreement with the resolution measured with a 5×5 matrix of PbF_2 crystals with the same cross section as the crystals used here [4]. Obviously the resolution is not limited by photoelectron statistics ($\sigma/E \approx 1/\sqrt{1600} \approx 2.5\%$ at 1 GeV, see Section 3.4). This is in qualitative agreement with Monte Carlo simulations.

5.2. Position resolution

We calculated the impact points of electromagnetic showers from the energy seen in the four PbF_2 crystals by using a logarithmic weighting method [8]: $\bar{x} = \sum w_i x_i / \sum w_i$, where the x_i denote the center coordinates of the four crystals and the weights w_i were calculated from the energies E_i detected in each crystal by $w_i = \max(0., 3.5 + \ln(E_i / \sum E_i))$. This impact point was compared to the extrapolation of a track measurement in the drift chamber in front of the crystals. The extrapolation determined the impact point on the crystal surface with a resolution of $(0.5 \pm 0.1) \text{ mm}$ in the vertical and horizontal plane. For electrons in the energy range from 1 to 6 GeV Fig. 7 shows the impact position calculated from the energy depositions in the calorimeter versus the extrapolation with the drift chamber data [9]. We had to restrict the analysis to an area of $10 \times 10 \text{ mm}^2$ in the center of the matrix. Otherwise systematic shifts of the reconstructed shower position from calorimeter information would occur because of lateral leakage. Within the experimental uncertainties no systematic deviation from linearity between both determinations is observed. To determine the position resolution of the calorimeter the resolution of the drift chamber extrapolation was subtracted quadratically from the difference between the impact points reconstructed with the crystals and with the drift chamber. With the 2×2 matrix we obtained a resolution of $\sigma_{x,y} = (0.99 \pm 0.06) \text{ mm} / \sqrt{E/\text{GeV}}$.

5.3. Spatial homogeneity

The spatial homogeneity of a PbF_2 matrix was measured by a scan over the surface of two adjacent crystals using electrons with energies between 1 and 6 GeV. The normalized mean values of the sum of the detected energy in the two crystals versus the extrapolated impact positions determined with the drift chamber data are plotted in Fig.

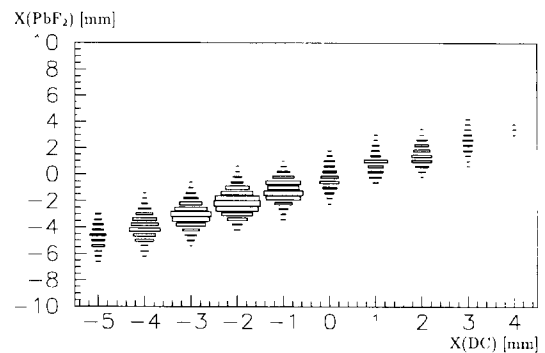


Fig. 7. The horizontal impact coordinates of electrons on the calorimeter surface reconstructed with the energy measurements versus extrapolations from drift chamber data. The PbF_2 matrix center is located at $x = 0 \text{ mm}$.

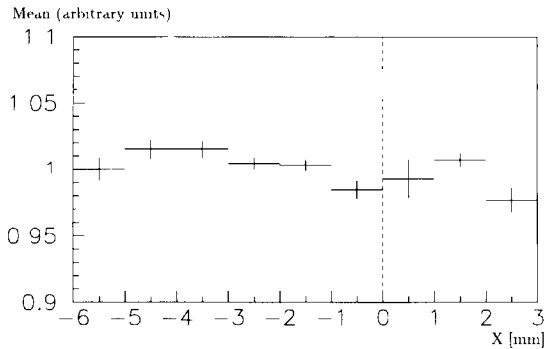


Fig. 8. The sum of the pedestal subtracted and normalized ADC counts of the signal seen in two crystals for a position scan between these crystals. The dashed line indicates the border between the crystals.

8. A systematic decrease of the mean value is explained by a non-perfect relative calibration of the photomultipliers. At the crack between the two crystals (indicated by the broken line in Fig. 8) the observed signal amplitude decreased by less than 1.5% while the r.m.s. of the energy distribution got worse by a factor of approximately 1.1.

5.4. Separation of electrons and pions

Fig. 9 shows the pulse height distribution for 5 GeV e^+ and π^+ beams hitting the center of the 2×2 matrix. Due to a different optical coupling as used in the DESY measurements (60 μm air gaps instead of optical grease) the CERN data show a different electromagnetic resolution. The beam spot extended over an area of 10×10 mm^2 . Clearly a peak of minimum ionizing particles (MIPs) is visible well separated from zero. Using electron calibration and correcting for the lateral leakage of electromagnetic showers the visible energy of MIPs corresponds to electrons with an energy of 110 MeV. From EGS simulations the energy deposition of MIPs is expected to be 200

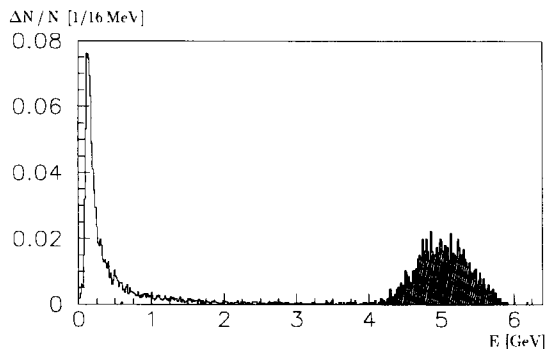


Fig. 9. The measured energy for 5 GeV π^+ (non shaded) and e^+ (shaded) beams hitting the center of the 2×2 matrix. Both distributions are normalized to the same area.

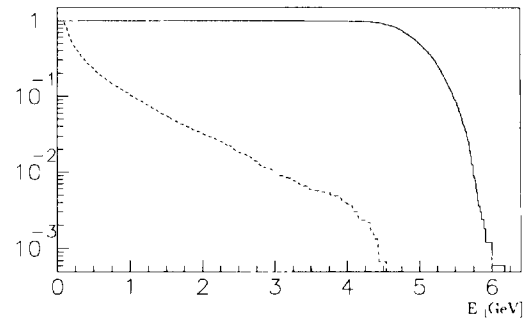


Fig. 10. The measured fraction of pions (broken line) and positrons (line) of 5 GeV momentum that are detected with an energy deposition larger than E in the PbF_2 calorimeter.

MeV. The difference is explained by different angular distributions of Cherenkov photons produced by MIPs and electromagnetic showers containing many charged particles, so that different fractions of the light are totally reflected at the crystal end facing the photomultiplier. Note that the scenario is different if optical grease is used to couple phototubes and crystals. Then more Cherenkov light of large angles with respect to the crystals end face is accepted and MIPs are measured with an energy near to their energy deposition [2,4].

If the momenta are known, pions can be suppressed by cutting on the energy detected in the PbF_2 crystals. At 5 GeV beam energy a cut keeping 90% of the positrons rejects more than 99.9% of the pions (Fig. 10). This separation gets worse with decreasing momenta, since the signals of interacting pions and electrons become less separated from the energy deposition of MIPs.

In addition the lateral spread of the showers can be used to distinguish interacting hadrons from electrons. We compared the response of 5 GeV e^+ and π^+ beams hitting an area of 10×10 mm^2 in the center of one crystal

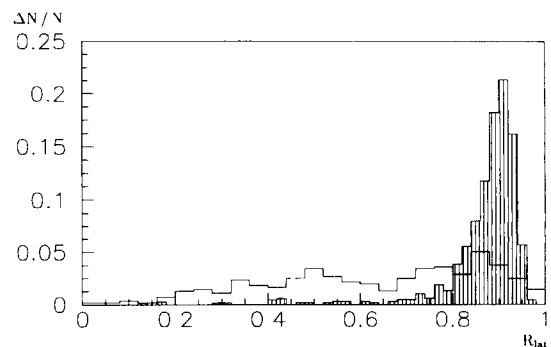


Fig. 11. The ratio R_{lat} of the energy measured in the crystal hit by a 5 GeV beam to the sum of the energies detected in all four crystals for e^+ (shaded) and π^+ (non shaded). Both distributions are normalized to the same area. Only particles with more than 650 MeV visible energy were taken into account.

to demonstrate that this procedure can also be applied efficiently with a PbF_2 calorimeter. In Fig. 11 the ratio R_{lat} of the signal seen in this crystal divided by the energy sum of all four crystals is plotted. Only events with total visible energy exceeding 650 MeV (well above the MIP peak) were taken into account. For positrons about 90% of the total visible energy stays in the hit crystal while pions show a broad distribution. For a ratio $R_{\text{lat}} > 0.8$ one keeps 90% of the positrons but rejects 70% of the interacting pions. This separation is expected to improve significantly when a larger PbF_2 matrix is used.

6. Outlook

Although the H1 collaboration will not realize the PbF_2 option, possible larger scale production of many PbF_2 crystals is presently being studied together with the Dr. Karl Korth oHG, Kiel, Germany. First experiences with PbF_2 raw material from Krasny Chemistry, St. Petersburg, Russia, show that it does not fulfill at present the stringent quality requirements, whereas Merck, Darmstadt, Germany, delivers raw material with sufficient purity for good crystals, but at a much higher price.

7. Summary

We have studied the use of PbF_2 crystals for calorimetry in high energy physics. The main features are excellent spatial homogeneity and good position and energy resolution for electromagnetic showers. Although the test module consisted of only four crystals electrons could already be separated from pions using the lateral shower measurement alone.

Radiation damage was cured by exposing PbF_2 crystals to daylight. The influence of spatial transmission variations and radiation damage on the performance of a lead fluoride calorimeter can be minimized when light with short wavelength is absorbed in a filter. Therefore we compared the performance of a PbF_2 crystal with and without a filter. When wavelengths shorter than 375 nm are cut off the electromagnetic energy resolution measured with an unradicated crystal was not deteriorated.

Acknowledgements

It is a pleasure to thank K. Thiele and G. Falley (DESY) for their permanent competent technical help. We are grateful to F. Kovacs, E. Barrelet, R. Zitoun (University of Paris VI and VII) and F. Moreau (Ecole Polytechnique, Palaiseau) for the setup of the CERN experiment and technical help. Z. Bryknar, P. Malek, M. Nikl, K. Polak, J. Pospisil, J. Walter and I. Wilhelm from the University of Prague, who participated in the optical measurements of the crystal properties, made it possible to understand the main features of the test beam data. We thank the staff off the CARY laboratory at the University of Dortmund for absorption measurements of PbF_2 crystals and D. Lauterjung of the University of Dortmund for providing us with a drift chamber. T. Mashimo from the OPAL collaboration supported this analysis with a program to simulate Cherenkov light tracking.

This work was supported by the Bundesministerium für Forschung und Technologie, Germany, under contract number 6DO57P (6).

References

- [1] A. Kantz, R. Hofstadter, *Nucleonics* 12 (1954) 36; E.B. Dally, R. Hofstadter, *Rev. Sci. Instr.* 39 (1968) 658; E.B. Dally, R. Hofstadter, *IEEE Trans. Nucl. Sci.* NS-15 (3) (1968) 76.
- [2] D.F. Anderson et al., *Nucl. Ins. and Meth. A* 290 (1990) 385.
- [3] Y. Kuno et al., TRIUMF Experiment 787, Technical Note No. 222 (1991).
- [4] C.L. Woody et al., *IEEE Trans. Nucl. Sci.* NS-40 (1992).
- [5] J. Janoth, diploma thesis, Universität Dortmund (1993), unpublished; J. Janoth et al., Response of Mesh-Type Photomultipliers in Strong Magnetic Fields, DESY-Report 93-119 (1993), submitted to *Nucl. Inst. and Meth.*
- [6] *Encycl. Dict. of Phys.*, Vol. 3, (Pergamon, 1961) p. 581.
- [7] H. Westermann, internal report DESY FCE 92-01.
- [8] T.C. Awes et al., *Nucl. Instr. and Meth. A* 311 (1992) 130.
- [9] S. Spielmann, diploma thesis, Universität Dortmund (1993), unpublished.